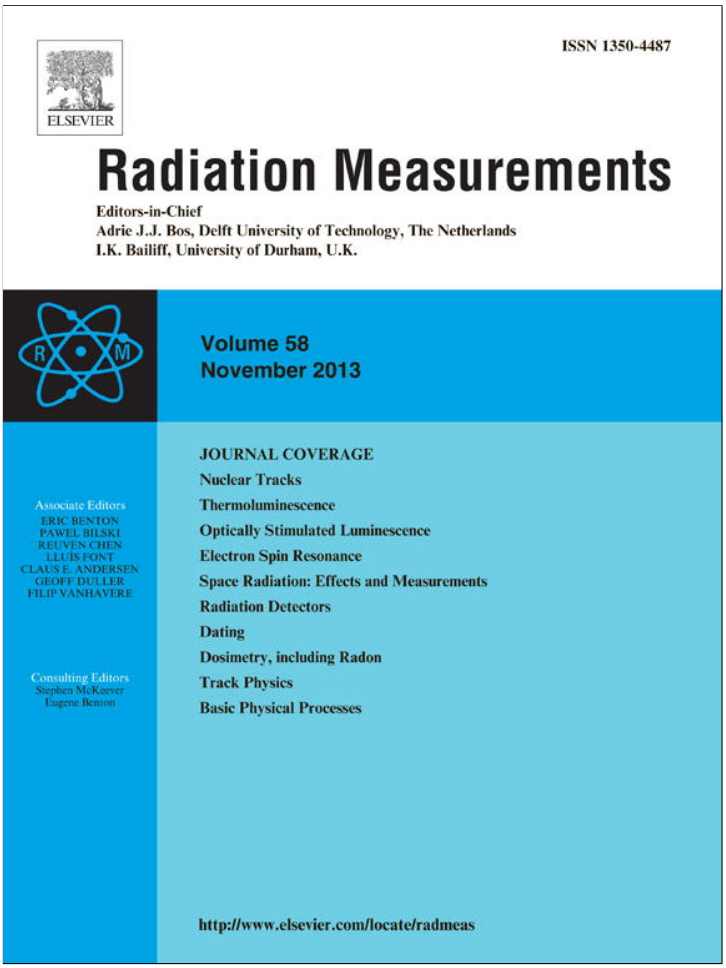

Radiation Measurements 58 (2013) 66–74

Contents lists available at ScienceDirect

Radiation Measurements

journal homepage: www.elsevier.com/locate/radmeas

Further investigations of tunneling recombination processes in random distributions of defects

Vasilis Pagonis [a,*], Huy Phan [a], David Ruth [a], George Kitis [b]

[a] Physics Department, McDaniel College, Westminster, MD 21157, USA
[b] Nuclear Physics Laboratory, Aristotle University of Thessaloniki, 54124 Thessaloniki, Greece

HIGHLIGHTS

- Further investigations of Tunneling model for feldspars.
- Approximate solutions are obtained for distribution of donors in the ground state.
- LM-IRSL signals in feldspars are analyzed using the model.
- Equations are tested by fitting LM-IRSL data for Na- and K-feldspar.

ARTICLE INFO

Article history:
Received 7 November 2012
Received in revised form
10 June 2013
Accepted 21 August 2013

Keywords:
Stimulated luminescence emission
Feldspars
Tunneling
Thermoluminescence
TL
Infrared stimulated luminescence
IRSL
OSL
Kinetic model
Random defect distribution

ABSTRACT

The shape of infrared stimulated luminescence signals (IRSL) from feldspars has been the subject of numerous studies in the field of luminescence dating. Specifically linearly modulated IRSL signals (LM-IRSL) are commonly assumed to consist of several first order components corresponding to distinct optical stimulation cross sections. This paper models the shape of LM-IRSL signals using a recently proposed kinetic model, which describes localized electronic recombination in donor–acceptor pairs of luminescent materials. Within this model, recombination is assumed to take place via the excited state of the donor, and nearest-neighbor recombinations take place within a random distribution of centers. The model has been used previously successfully to describe both thermally and optically stimulated luminescence (TL, OSL). This paper shows that it is possible to obtain approximate solutions for the distribution of donors in the ground state as a function of two variables, time and the distance between donors and acceptors. Approximate expressions are derived for several possible modes of optical and thermal stimulation, namely TL, OSL, linearly modulated OSL (LM-OSL), LM-IRSL and isothermal TL (ITL). Numerical integration of these expressions over the distance variable yields the distribution of remaining donors at any time t during these experimental situations. Examples are given for the derived distributions of donors in each experimental case, and similarities and differences are pointed out. The paper also demonstrates how LM-IRSL signals in feldspars can be analyzed using the model, and what physical information can be extracted from such experimental data. The equations developed in this paper are tested by fitting successfully a series of experimental LM-IRSL data for Na- and K-feldspar samples available in the literature. Finally, it is shown that the equations derived in this paper are a direct generalization of an equation previously derived for the case of ground state tunneling.

1. Introduction

Localized transition recombination models (LTM) have been used extensively to describe a variety of behaviors of luminescence signals and in a wide variety of materials (see for example the books by Chen and McKeever (1997), Bøtter-Jensen et al. (2003) and Chen and Pagonis (2011)). These models are based on the assumption of a fixed recombination probability between the excited state of a trap and a recombination center (Chen, 1976; Bull, 1989; Mandowski, 2005; Sunta et al., 2006; Kumar et al., 2006, 2007). However, recent experimental and modeling studies support the notion that the recombination probability for localized transitions in many materials, such as feldspars, may vary with time (Thomsen et al., 2011; Jain and Ankjærgaard, 2011; Jain et al., 2012; Andersen et al., 2012).

* Corresponding author. Tel.: +1 410 857 2481; fax: +1 410 386 4624.
E-mail address: vpagonis@mcdaniel.edu (V. Pagonis).

1350-4487/$ – see front matter © 2013 Elsevier Ltd. All rights reserved.
http://dx.doi.org/10.1016/j.radmeas.2013.08.006

Quantum mechanical tunneling and the associated phenomenon of "anomalous fading" of luminescence signals in feldspar has received a lot of attention, due to the importance of this phenomenon in dating studies (Templer, 1986; Visocekas, 1985; Duller and Bøtter-Jensen, 1993; Visocekas et al., 1994; Murray et al., 2009, and references therein). Several studies have suggested that anomalous fading is due to quantum mechanical tunneling from the ground state of the trap (Huntley and Lamothe, 2001; Poolton et al., 2002a, 2002b; Li and Li, 2008, 2010; Kars et al., 2008; Larsen et al., 2009). Furthermore, it has been shown that the ground state tunneling process in various materials can be described by a power-law type of decay (Delbecq et al., 1974; Baril, 2002; Baril and Huntley, 2003; Huntley, 2006). The experimental and modeling work by Poolton et al. (2002a, 2002b, 2009) and more recently by Jain and Ankjærgaard (2011) and Ankjærgaard et al. (2009), provided valuable information on the origin of infrared stimulated luminescence (IRSL) from feldspars, and supported the existence of tunneling processes involving localized recombinations taking place from the excited state of the trap, as well as charge migration through the conduction band-tail states. In a recent paper Pagonis et al. (2012) presented a new empirical kinetic model based on localized electronic transitions, in an attempt to describe such tunneling via the excited state in feldspars. The continuous-wave IRSL signals (CW-IRSL) from feldspars are known to decay in a non-exponential manner and the exact mathematical shape of these curves is an open research question (Thomsen et al., 2008, 2011). Bailiff and Poolton (1991) and Baril (2002) showed that the IRSL decay follows a power law, while Poolton et al. (2002a, 2002b) explained IRSL in feldspars using a donor–acceptor model, in which electron tunneling occurs from the excited state and the band tail states of the IRSL trap. Extensive linearly-modulated IRSL work (LM-IRSL) on feldspars was also carried out by Fattahi and Stokes (2003, 2006). Thomsen et al. (2011) suggested that the beginning of the IRSL decay curve originates with the luminescence emitted from close donor–acceptor pairs, while the end of the IRSL curve most likely represents the tunneling of distant pairs.

In a recent important development in this research area, Jain et al. (2012) presented a new kinetic model which quantifies localized electronic recombination of donor–acceptor pairs in luminescent materials. Recombination is assumed to take place via the excited state of the donor, and only for nearest-neighbors within a random distribution of centers. Two versions of the model were presented, an exact model that evolves in both space and time, and an approximate semi-analytical model evolving only in time. These authors found good agreement between the two versions of their models, and simulated successfully both thermally stimulated luminescence (TL) and optically stimulated luminescence (OSL). Their model also demonstrated the power law behavior for OSL signals. The semi-analytical version of the model by Jain et al. (2012) was examined by Kitis and Pagonis (2013), who showed that the system of simultaneous differential equations can be approximated to a very good precision by a single differential equation. These authors obtained analytical solutions for this single differential equation, and for four different experimental modes of stimulation: TL, OSL, linearly modulated OSL (LM-OSL) and isothermal TL processes.

The present paper is concerned with the exact version of the model developed by Jain et al. (2012), instead of the semi-analytical version of the model studied by Kitis and Pagonis (2013).

The goals of the present paper are:

(a) To show that the time dependence of the equations developed by Jain et al. (2012) can be integrated analytically, and that the behavior of the system is described by an integral equation over the distance variable only.
(b) To obtain approximate solutions for the distribution of donors in the ground state as a function of time and of the distance between the donor–acceptor pairs. These expressions are derived for several possible modes of stimulation, namely TL, OSL, LM-OSL (and LM-IRSL), and isothermal TL (ITL).
(c) To demonstrate how typical LM-IRSL signals can be analyzed using the model of random defects interacting via the tunneling mechanism, and what physical information can be extracted from such experimental data.
(d) To test the equations developed in this paper by fitting a series of experimental LM-IRSL data for Na- and K-feldspar samples available in the literature.
(e) To show that the equations derived in this paper are a generalization of the equation derived by Huntley (2006) for the case of ground state tunneling.

2. Description of the physical system and model by Jain et al. (2012)

The physical assumptions in the model of Jain et al. (2012) are summarized in Table 1 of their paper. The main physical assumption in the model is the presence of a random distribution of hole traps in the luminescent volume, and an associated range of random nearest-neighbor recombination probabilities. Furthermore, stimulated recombination takes place only via the excited state of the electron trap, by either optical or thermal stimulation. The concentration of holes is assumed to be much larger than the concentration of electron traps, and an electron can tunnel only to its nearest hole. In the exact form of the model presented by Jain et al. (2012), the differential equations are:

$$\frac{\partial n_g(r',t)}{\partial t} = -An_g(r',t) + Bn_e(r',t), \tag{1}$$

$$\frac{\partial n_e(r',t)}{\partial t} = An_g(r',t) - Bn_e(r',t) - \frac{n_e(r',t)}{\tau(r',t)}, \tag{2}$$

$$L(t) = -\frac{dm}{dt} = \int_0^\infty \frac{n_e(r',t)}{\tau(r',t)} dr' = -\int_0^\infty \left(\frac{\partial n_g(r',t)}{\partial t} + \frac{\partial n_e(r',t)}{\partial t}\right) dr', \tag{3}$$

$$\begin{matrix} \frac{dT}{dt} = \beta \quad (\text{for TL}) \\ \frac{dT}{dt} = 0 \quad (\text{for isothermal TL, CW} - \text{OSL and LM} - \text{OSL}) \end{matrix}, \tag{4}$$

$$\tau = s^{-1}\exp\left(\frac{r'}{(\rho')^{1/3}}\right). \tag{5}$$

The following parameters and symbols are used in the model: $n_g(r',t)$ and $n_e(r',t)$ are the instantaneous concentrations of electrons in the ground state and in the excited state correspondingly. These concentrations depend on both time t and on the dimensionless separation distance parameter r' which is defined by $r'=(4\pi\rho/3)^{1/3}r$, where r represents the actual donor–acceptor separation distance. The dimensionless number density of acceptors parameter ρ' is defined by $\rho'=(4\pi\rho/3)\alpha^{-3}$, where ρ represents the actual number density of acceptors and α is the potential barrier penetration constant (Huntley, 2006). m is the instantaneous concentration of acceptors (holes), n is the instantaneous concentration of all the

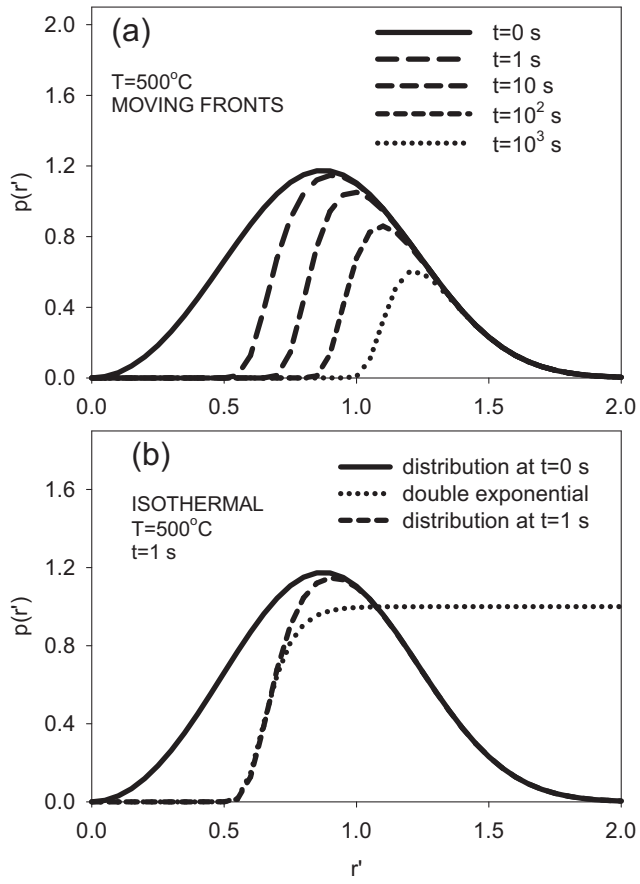

Fig. 1. (a) Examples of the distribution of electrons in the ground state $n_g(r',t)$ from equation (20), for the case of isothermal TL experiments at a temperature of $T = 500$ °C, and at different times t from the start of the experiment. The parameters used are $E = 1.2$ eV, $s = 10^{12}$ s^{-1}, and $\rho' = 3\times10^{-4}$. (b) Example of the three functions in equation (20) discussed in the text: the "moving tunneling front" in the isothermal process (dashed line), the sharp rising double exponential function (dotted line) and the peak-shaped distribution function (solid line). These three functions are shown for time $t = 1$ s after the start of the isothermal experiment.

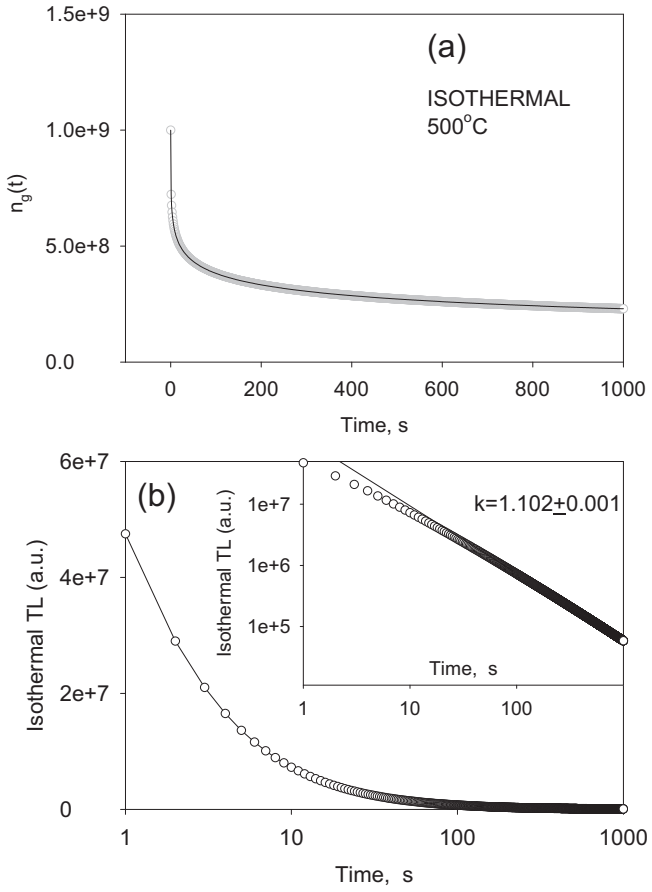

Fig. 2. (a) The concentration $n_g(t)$ of remaining electrons in the ground state, obtained by numerically integrating equation (20) over the possible range of values of normalized distances $r' = 0$–2. The solid line is the exact solution of equations (1)–(5) with no approximations. (b) The luminescence intensity $L(t)$ obtained by numerically evaluating the derivative of the concentrations shown in (a). The same data is shown in the inset on a log–log scale, demonstrating the power law with a coefficient $k = 1.102 \pm 0.001$.

donors, and N represents the instantaneous concentration of electrons in thermally disconnected states, such that charge is conserved, i.e. $m = n+N = (n_g + n_e) + N$. It is noted that the variables m and r' are not independent, but they are directly related; if the concentrations n_g,n_e are known as a function of time, then m can also be calculated as a function of time via this charge conservation equation. The parameter A represents the excitation rate from the ground to the excited state, and is equal to $A = sexp(-E/kT)$ and $A = \sigma(\lambda)I$ for the cases of thermal and optical excitation correspondingly. Here E = thermal activation energy, s is the frequency factor, β is the linear heating rate, λ is the optical stimulation wavelength, $\sigma(\lambda)$ is the optical absorption cross-section and I is the light intensity. Additional parameters in equation (5) are the dimensionless number density of acceptors ρ', and τ is the tunneling lifetime. B is the relaxation rate from the excited into the ground state, and $L(t)$ is the instantaneous luminescence resulting from recombination taking place via the excited state. If the equivalence principle is assumed to be valid, one also has $B = s$. However, this is not a necessary condition for obtaining the approximate solutions in this paper.

Jain et al. (2012) developed also an approximate semi-analytical model to describe the behavior of the system. This second version of the model evolves only in time, and the approximation is based on introducing a critical tunneling lifetime τ_c. These authors found good agreement between the exact and the approximate semi-analytical version of their model, and simulated successfully both thermally stimulated luminescence (TL) and optically stimulated luminescence (OSL). The model also demonstrated the power law behavior for simulated OSL and ITL signals. However, the approximate semi-analytical model was found to disagree with the exact solution of the model in the case of low values of the optical excitation probabilities $A = 1$–10 s^{-1} (Jain et al. (2012), their figure 7a and 7b).

In the next section a partial analytical solution is obtained for the system of equations in the original model of Jain et al. (2012). The derivation proceeds as follows:

(a) Firstly an approximate equation is derived which describes the distribution of donors in the ground state, as a function of both time and distance (t and r' respectively).
(b) Secondly, specific forms of this equation are developed, which are applicable for several possible experimental situations involving either optically or thermally stimulated luminescence.
(c) Next, by numerically integrating the derived equation over the distance variable r', the distribution of remaining donors is obtained at any time t. Examples are given for the distributions of donors for several types of experiments.

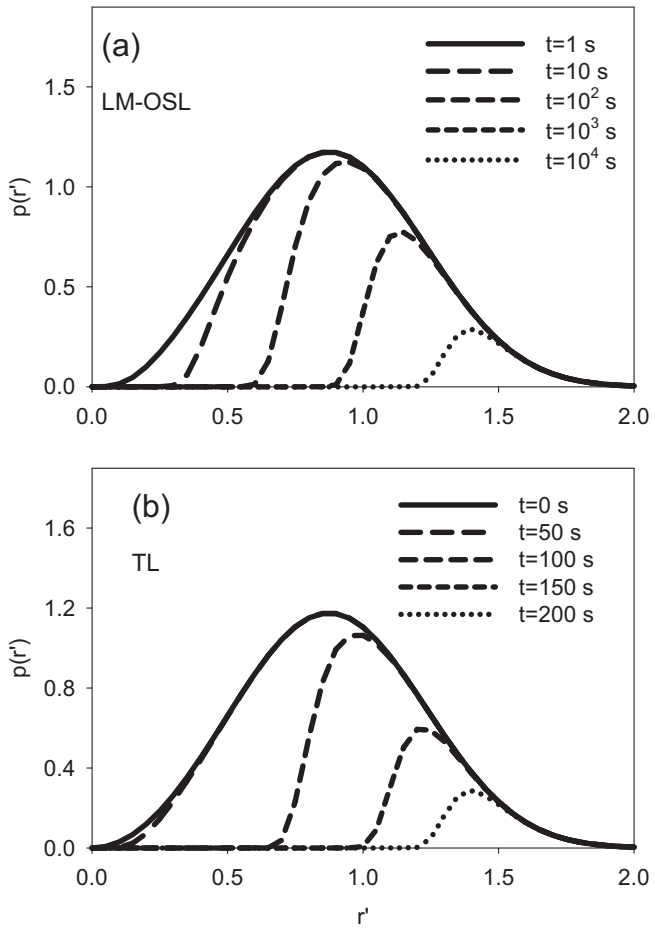

Fig. 3. (a) Examples of the analytical equation (22), for the case of LM-OSL (or LM-IRSL) experiments. The parameters used in this simulation are $b = 10\ s^{-1}$, $T = 3000$ s, $B = s = 10^{12}\ s^{-1}$ and $\rho' = 3\times10^{-4}$. The "moving tunneling fronts" for $n_g(r',t)$ during the LM-OSL experiment are seen for several times $t = 0$–10^4 s from the start of the experiment. (b) Examples of the analytical equation (25), at several times t from the start of the TL experiment. The parameters used are $E = 1.2$ eV, $s = 10^{12}\ s^{-1}$, and $\rho' = 3\times10^{-4}$.

(d) Finally, by numerically calculating the derivative of the distributions in part (c) with respect to time t, the luminescence intensity $L(t)$ is obtained as a function of time.

3. Approximate solutions of the exact model by Jain et al

Jain et al. (2012, their Fig. 4(b)) showed that for typical numerical values of the parameters in the model, n_e is many orders of magnitude smaller than n_g. Careful consideration of the numerical solutions of the system of equations (1)–(4) shows that the numerical values of the term $\partial n_e(r',t)/\partial t$ on the left hand side of equation (2) is many orders of magnitude smaller than either of the terms $An_g(r',t)$ and $-Bn_e(r',t) - n_e(r',t)/\tau(r',t)$ on the right hand side of this equation. On the basis of this observation (which is verified for a wide range of values of the parameters in the model), one can set

$$\frac{\partial n_e(r',t)}{\partial t} \approx 0, \tag{6}$$

and hence equation (2) can be solved for n_e to yield:

$$n_e(r',t) = \frac{An_g(r',t)}{B + \frac{1}{\tau(r',t)}}. \tag{7}$$

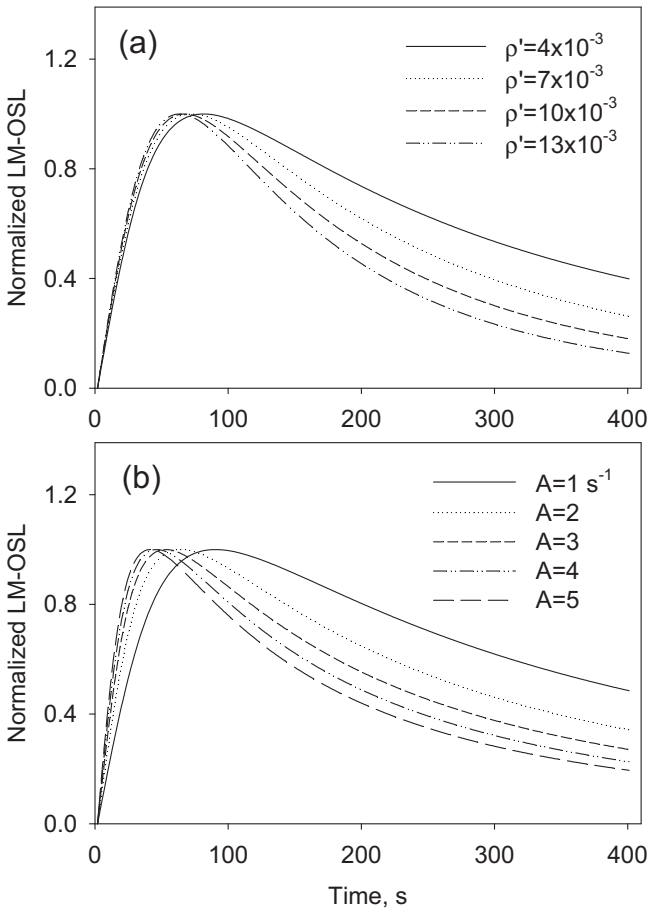

Fig. 4. The effect of the parameters (a)ρ' (normalized charge density), and (b) A (optical stimulation probability) on the shape of simulated LM-IRSL signals. The signals shown have been normalized to the maximum intensity for comparison purposes.

It is noted that from a strictly mathematical point of view, the condition $\partial n_e(r',t)/\partial t \approx 0$ used here is a rather ad-hoc assumption, which is eventually justified from the numerical results of the simulation. It is possible that in a different physical system this assumption may not be valid. However, from a physical point of view one might expect that excited states in feldspar relax quite rapidly compared to the time scales of TL and OSL experiments, and therefore the time scale for electronic relaxation processes involving the excited states (term $\partial n_e/\partial t$ in equation (2)) can be of the order of ns or μs, while the time scale for TL processes can be of the order of ms or s. It is noted that a mathematically similar approximating method was used in the recent paper by Chen et al. (2012), to obtain semi-analytical solutions for a different system of differential equations.

Substituting equation (7) into (1) one obtains:

$$\frac{\partial n_g(r',t)}{\partial t} = -An_g(r',t) + B\frac{An_g(r',t)}{B + \frac{1}{\tau(r',t)}} = \frac{-An_g(r',t)}{B\tau(r',t) + 1}. \tag{8}$$

For typical physically reasonable values of the parameters, the numerical value of the quantity $B\tau(r',t)$ in the denominator of this equation is much larger than 1, hence we can approximate

$$\frac{\partial n_g(r',t)}{\partial t} = \frac{-An_g(r',t)}{B\tau(r',t)}. \tag{9}$$

Substituting equation (5) into (9):

$$\frac{\partial n_g(r',t)}{\partial t} = \frac{-An_g(r',t)}{Bs^{-1}\exp\left(\frac{r'}{(\rho')^{1/3}}\right)} = \frac{-An_g(r',t)}{\exp\left(\frac{r'}{(\rho')^{1/3}}\right)}, \tag{10}$$

where the equivalence principle $B = s$ was used. The parameter A can be a function of time, and depends on the type of stimulation mode used during the experiment.

Equation (10) can be considered a partial differential equation with respect to the time variable t. This equation can be formally integrated (by assuming a fixed distance r') with respect to time t, to yield a decaying exponential function $n_g(r',t)$ which varies with time t according to:

$$n_g(r',t) = n_g(r',0)\exp\left[-\exp\left(-(\rho')^{-1/3}r'\right)\int_0^t A\mathrm{d}t'\right], \tag{11}$$

where $n_g(r',0)$ represents the initial concentration of electrons in the ground state at time $t = 0$ corresponding to a distance r' between the donor and acceptor. As discussed in Jain et al. (2012, their equation (6)), this initial distribution of electrons in the ground state at time $t = 0$ is given by the peak-shaped probability density function (PDF):

$$n_g(r',0) = 3n_0(r')^2\exp\left[-(r')^3\right]. \tag{12}$$

Finally by combining (11) and (12) one obtains the desired partial analytical solution:

$$n_g(r',t) = 3n_0(r')^2\exp\left[-(r')^3\right]\exp\left[-\exp\left(-(\rho')^{-1/3}r'\right)\int_0^t A\mathrm{d}t'\right]. \tag{13}$$

Equation (13) describes the evolution of the distribution of electrons in the ground state as a function of the time t elapsed since the beginning of the optical or thermal stimulation. It is valid for several types of excitation used in typical TL or OSL experiments. As discussed in subsequent sections, the integral $\int_0^t A\mathrm{d}t'$ can be evaluated for the different excitation modes, and it is possible to obtain a closed approximate form for the distribution $n_g(r',t)$ in equation (13). It is noted that the same integral appears in the analytical equation developed in Kitis and Pagonis (2013), who examined the semi-analytical version of this model.

By integrating equation (13) over the distance variable r', one finds the remaining number of electrons in the ground state at time t :

$$n_g(t) = \int_0^2 3n_0(r')^2\exp\left[-(r')^3\right]\exp\left[-\exp\left(-(\rho')^{-1/3}r'\right)\int_0^t A\mathrm{d}t'\right]dr'. \tag{14}$$

The time-dependent luminescence intensity $L(t)$ is evaluated from equation (3). By using the approximations $n_e << n_g$, $n_e + n_g \approx n_g$, and $\frac{\partial n_e(r',t)}{\partial t} << \frac{\partial n_g(r',t)}{\partial t}$ one obtains:

$$L(t) = \int_0^\infty \frac{n_e(r',t)}{\tau(r',t)}\mathrm{d}r' = -\int_0^\infty\left(\frac{\partial n_g(r',t)}{\partial t} + \frac{\partial n_e(r',t)}{\partial t}\right)\mathrm{d}r' \approx -\int_0^\infty\left(\frac{\partial n_g(r',t)}{\partial t}\right)\mathrm{d}r', \tag{15}$$

or by substituting (13) into (15):

$$L(t) \approx -\int_0^\infty \frac{\partial n_g(r',t)}{\partial t}\mathrm{d}r' = -\int_0^\infty \frac{\partial}{\partial t}\left[n_g(r',0)\exp\left[-\exp\left(-(\rho')^{-1/3}r'\right)\int_0^t A\mathrm{d}t'\right]\right]\mathrm{d}r'. \tag{16a}$$

By carrying out the differentiation symbolically:

$$L(t) = \int_0^\infty A\exp\left(-(\rho')^{-1/3}r'\right)n_g(r',0)\exp\left[-\exp\left(-(\rho')^{-1/3}r'\right)\int_0^t A\mathrm{d}t'\right]\mathrm{d}r'. \tag{16b}$$

This integral expression allows a numerical calculation of the luminescence intensity $L(t)$, by integrating numerically over the possible range of the dimensionless variable $r' = 0$ to $r' = \infty$.

Although it is not possible to obtain a closed analytical form of the luminescence intensity $L(t)$ as a function of time, $L(t)$ can be easily evaluated by numerically integrating equation (16b) over the distance r'.

3.1. Discussion of equation (14)

It is instructive to compare equation (14) with the equation derived by Huntley (2006) for the case of ground state tunneling. During an isothermal TL, a CW-OSL or a CW-IRSL experiment the probability A of excitation into the excited state is constant with time, so that $\int_0^t A\mathrm{d}t' = At$ and equation (14) becomes:

$$n_g(t) = \int_0^\infty 3n_0(r')^2\exp\left[-(r')^3\right]\exp\left[-\exp\left(-(\rho')^{-1/3}r'\right)At\right]\mathrm{d}r'. \tag{17}$$

By substituting equation (5) for the tunneling lifetime into equation (17), it becomes:

$$n_g(t) = \int_0^\infty 3n_0(r')^2\exp\left[-(r')^3\right]\exp\left[-\frac{At}{s\tau}\right]\mathrm{d}r'. \tag{18}$$

This equation is identical in form to the following expression derived by Huntley (2006), equation (4) in that paper:

$$\frac{n(t)}{n_o} = \int_0^\infty 3(r')^2\exp\left[-(r')^3\right]\exp[-t/\tau]\mathrm{d}r', \tag{19}$$

with the quantity $\tau_{eff}=(s\tau/A)$ in equation (18) representing an "effective lifetime" for stimulation into the excited state, and the subsequent recombination process.

It is concluded that equation (18) in this paper is a direct generalized form of equation (4) in the work by Huntley (2006). While the Huntley equation is applicable for ground state tunneling, equation (18) in this paper is more general and can describe tunneling from the excited state of the physical system. Most importantly, equation (18) can be used to describe the time variation of the concentration of donors during various cases of optical or thermal excitation.

3.2. Isothermal TL, CW-OSL and CW-IRSL experiments

In the case of isothermal TL experiments (ITL), the quantity $A=sexp(-E/kT_o)$ = constant, where T_o is the temperature at which the isothermal experiment is carried out. From equation (13) one finds:

$$n_g(r',t) = 3n_0(r')^2 \exp\left[-(r')^3\right]\exp\left[-\exp\left(-(\rho')^{-1/3}r'\right)st\exp(-E/kT_o)\right]. \quad (20)$$

Fig. 1(a) shows examples of the distribution of electrons in the ground state $n_g(r',t)$ obtained using equation (20), for the case of isothermal TL experiments. The distributions $n_g(r',t)$ are shown for isothermal TL signals measured at a temperature of $T = 500$ °C, and at different times t from the start of the experiment. The parameters used in this simulation are activation energy $E = 1.2$ eV, frequency factor $s = 10^{12}$ s^{-1}, and the dimensionless number density of acceptors $\rho' = 3\times10^{-4}$.

The rising part of the curves in Fig. 1(a) represents the "moving tunneling front" in the isothermal process, which were discussed in some detail in Huntley (2006) for the case of ground state tunneling. These can be compared with the corresponding fronts for ground state tunneling shown in Fig. 1 of Huntley (2006). The rather sharp rising part in the functions in Fig. 1(a) is due to the double exponential function in equation (20). This double exponential function is multiplied by the peak-shaped distribution function $3(r')^2\exp[-(r')^3]$ in equation (20), resulting in the characteristic shape of the "moving front". These three functions are shown in Fig. 1(b) for time $t = 1$ s after the start of the isothermal experiment. In the approximate semi-analytical version of the model of Jain et al. (2012), one introduces a critical lifetime and a corresponding critical radius which describe the behavior of the physical system.

Fig. 2(a) shows the corresponding concentration $n_g(t)$ of remaining electrons in the ground state, which is obtained by numerically integrating equation (20) over the possible range of values of normalized distances $r'=0-2$. As seen in this figure, there are still about 25% of electrons remaining in the ground state of the system, even after $t = 1000$ s from the start of the experiment. The solid line in Fig. 2(a) is the exact solution of equations (1)–(5) in this paper describing the original model of Jain et al. (2012), with no approximations. Good agreement is seen between the numerical solution of equations (1)–(5) and equation (20) derived in this paper.

Fig. 2(b) shows the corresponding luminescence intensity $L(t)$, which is obtained by numerically evaluating the derivative of the concentrations shown in Fig. 2(a). The same data is shown in the inset of Fig. 2(b) on a log–log scale; at large times $t > 100$ s the data behaves linearly on a log–log scale (solid line), and they fit a power law with a coefficient $k = 1.102 \pm 0.001$. This is in agreement with the simulations of Jain et al. (2012) and Kitis and Pagonis (2013), who showed that for large times t the CW-OSL, IRSL and isothermal TL data should follow a modified power law of the form $L(t) \propto 1/t^k$, with a power law coefficient k very close to unity.

The case of CW-OSL or CW-IRSL excitation mode is similar to the isothermal TL experiments, with $A=\lambda$ = constant representing the optical excitation probability. From equation (13) one finds:

$$n_g(r',t) = 3n_o(r')^2\exp\left[-(r')^3\right]\exp\left[-\exp\left(-(\rho')^{-1/3}r'\right)\lambda t\right]. \quad (21)$$

Kitis and Pagonis (2013) showed analytically that the simulated luminescence intensity $L(t)$ in these two cases of CW-OSL or CW-IRSL excitation mode, follows the power law of luminescence for large times t, with the power law coefficient k very close to unity.

3.3. LM-OSL and LM-IRSL experiments

In the case of linearly modulated OSL (LM-OSL) and LM-IRSL excitation modes, the probability of optical excitation is varied linearly with time in the form $A = bt/T$, where T = total excitation period and b is a constant. In this case equation (13) becomes:

$$\frac{n_g(r',t)}{n_o} = 3(r')^2\exp\left[-(r')^3\right]\exp\left[-\exp\left(-(\rho')^{-1/3}r'\right)\frac{bt^2}{T}\right]. \quad (22)$$

Fig. 3(a) shows examples of equation (22), for the case of LM-OSL or LM-IRSL experiments. The parameters used in this simulation are $b = 10$ s^{-1}, $T = 3000$ s, $B = s = 10^{12}$ s^{-1} and the dimensionless number density of acceptors $\rho' = 3\times10^{-4}$. The "moving tunneling fronts" for $n_g(r',t)$ during the LM-OSL experiment are seen in Fig. 3(a) for several times $t = 0-10^4$ s from the start of the experiment.

Fig. 4 shows the effect of the parameters ρ' and A on the shape of LM-IRSL signals. The simulated LM-IRSL signals in Fig. 4 were normalized to the maximum intensity for clarity. Fig. 4(a) shows that the charge density ρ' affects mostly the "tail" of the LM-IRSL signals, while it also has a smaller effect on the rising part of the curve and on the peak location. The simulation in Fig. 4(b) shows that the optical probability A affects rather strongly all parts of the LM-IRSL curve: the rising part, "long tail" and the peak location.

3.4. Thermal excitation with a linear heating rate

In the case of heating with a linear heating rate β, the temperature varies as $T = T_o+\beta t$ where T_o is the room temperature and t is the time. In this case the integral appearing in equation (13) becomes:

$$\int_0^t A\,dt' = \int_0^t s\exp(-E/kT)\,dt' = \int_0^t s\exp\left[-\frac{E}{k(T_o+\beta t')}\right]dt'. \quad (23)$$

This expression is the well-known exponential integral of TL theory, which can be approximated accurately by the first two terms of its series (see for example the book by Chen and Pagonis (2011), Chapter 15):

$$\int_0^t A\,dt' = \frac{skT^2}{\beta E}e^{-\frac{E}{kT}}\left(1-\frac{2kT}{E}\right). \quad (24)$$

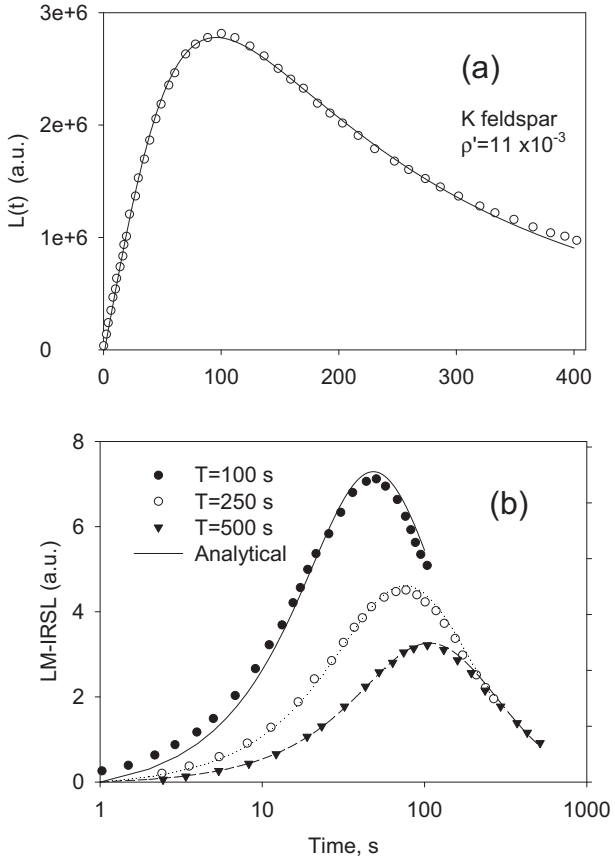

Fig. 5. (a) The experimental LM-IRSL data for K-feldspar from Bulur and Goksu (1999) are fitted using the analytical solution derived in this paper (solid line). (b) The LM-IRSL data of Bulur and Goksu (1999) in which they changed the ramping time T, while keeping the LED intensity fixed. The solid lines represent the simulated results as discussed in the text.

In this case equation (13) becomes:

$$\frac{n_g(r',t)}{n_o} = 3(r')^2 \exp\Big[-(r')^3\Big] \exp\Big[-\exp\Big(-(\rho')^{-1/3} r'\Big) \frac{skT^2}{\beta E} e^{-\frac{E}{kT}} \Big(1 - \frac{2kT}{E}\Big)\Big]$$
$$T = T_o + \beta t \qquad (25)$$

Expression (25) gives the instantaneous distribution $n_g(r',t)$ of electrons in the ground state at temperature T (or time t), during a TL experiment carried out with a constant heating rate β. Fig. 3(b) shows examples of equation (25), at several times t from the start of the TL experiment. The parameters used in this simulation are activation energy $E = 1.2$ eV, frequency factor $s = 10^{12}$ s^{-1}, heating rate $\beta = 5$ K/s and the dimensionless number density of acceptors $\rho' = 3\times10^{-4}$.

4. Comparison of derived equations with experimental data

In this section we give several examples of fitting experimental LM-IRSL data for feldspars using the equations in this paper.

Figs. 5 and 6 reproduce the experimental LM-IRSL data for two feldspar samples studied by Bulur and Goksu (1999). These authors studied fine powders of K and Na feldspar standards (samples NBS-70a and NBS-99a) by using IR LEDs with a light intensity of 40 mW/cm^2. The sensitivity of the samples was monitored using the corresponding TL signal, and was found to remain constant during the experiments. Fig. 5(a) in this paper shows the LM-IRSL data in Fig. 1(a) of Bulur and Goksu (1999), obtained after a dose of 11.25 Gy and a preheat of 5 min at 200 °C to remove the unstable components. The LM-IRSL signal from Na-feldspar was found to be much more intense than the corresponding output from the K-feldspar, and the peak maximum from Na-feldspar occurred at a shorter time. These authors fitted both signals using three first order components, each with a distinct optical cross section.

The solid line in Fig. 5(a) represents the solution in equation (22) derived in this paper, showing good agreement with the experimental data. The parameters used in this simulation are $b = 0.5$ s^{-1}, $T = 400$ s and the dimensionless number density of acceptors $\rho' = 11\times10^{-3}$. In another series of LM-IRSL measurements, Bulur and Goksu (1999) changed the ramping time T of the LM-IRSL experiment, while keeping the LED intensity fixed. A measurement of the TL signal after each measurement ensured that there were no appreciable changes in the sensitivity of the sample. The results of their measurements are reproduced in Fig. 5(b), together with the results of carrying out the simulation with a variable period T in equation (22) while keeping all other parameters fixed. Once more, reasonably good agreement is seen between the simulation and the experiment.

One uncertain factor in fitting the sets of data in Figs. 5–6 of this paper is the magnitude of the background signal during the LM-IRSL signal, since Bulur and Goksu (1999) did not report on its size. The fits shown in Figs. 5–6 assume that the background signal is negligible, an assumption that may or may not be correct. Another fact that may be influencing the accuracy of the fits in these Figures is the scattering in the original data.

In a third series of experiments, Bulur and Goksu studied the effect of increasing the stimulation temperature. The IR-stimulated luminescence in Na- and K-feldspars is enhanced by increasing the sample temperature and the activation energy for this process can be estimated by using an Arrhenius plot (Hutt et al. (1988); Hutt and Jaek, 1993; Bailiff and Poolton (1991); Bøtter-Jensen et al. (1994); Duller (1997). This activation process has been explained previously using a two-stage excitation of trapped electrons, with the first stage from the ground state into a meta-stable excited state by photon absorption, and in the second stage absorption of phonons causing release of electrons into the conduction band.

In a fourth experiment Bulur and Goksu (1999) measured the LM-IRSL signal of the two feldspar samples sequentially 15 times, and their data are reproduced in Fig. 6 of this paper. By the time the signal was measured for the 15th time, the observed luminescence curve was reduced to a line. The results of the experiment showed that the first measurement was relatively intense and contained a peak structure with the maximum occurring at relatively short times. In the second and the following LM-IRSL measurements the luminescence output decreased gradually and the peak position shifted to longer times, as seen in Fig. 6(a). Bulur and Goksu

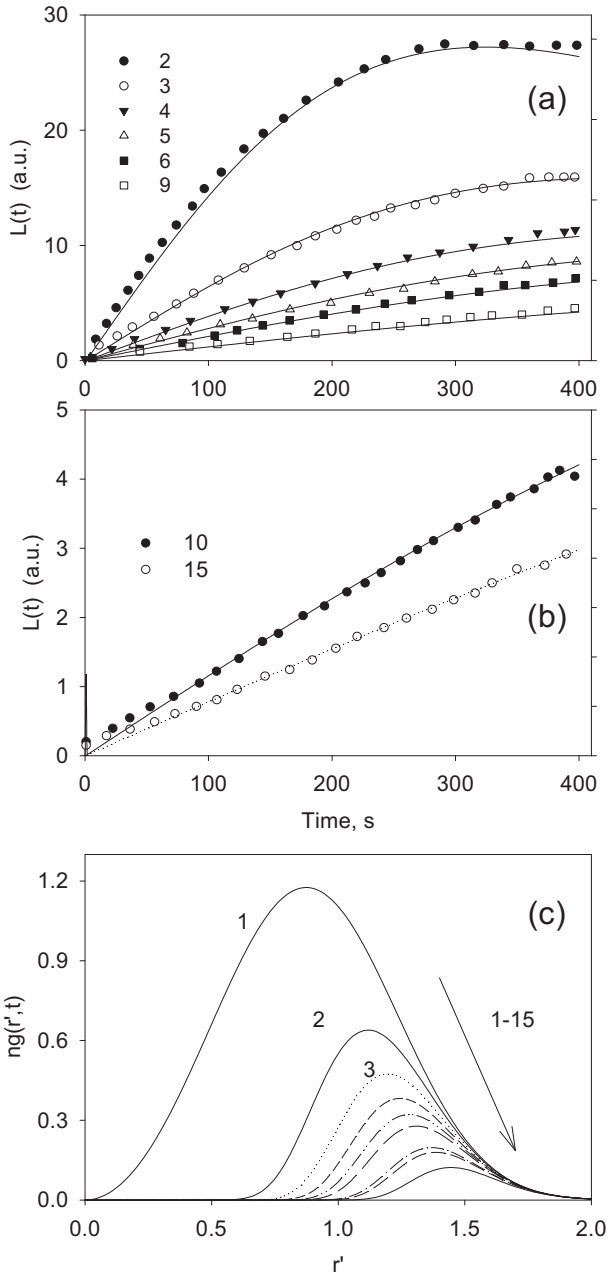

Fig. 6. (a) The sequential data of Bulur and Goksu (1999) obtained in their sequence 2–9. Their first LM-IRSL measurement was shown as the solid curve in Fig. 5b. The solid lines indicate the simulation results, as discussed in the text. (b) Sequences 10 and 15 of the data of Bulur and Goksu (1999). (c) The simulated "tunneling fronts" for sequences 1–15 shown in (a) and (b).

interpreted and fitted their data by assuming the presence of three separate first order components. They concluded that the third component of the signal was partially depleted by the first measurement.

In this paper we offer an alternative explanation of the behavior seen in the data of Bulur and Goksu (1999), by using the following simulation procedure. The result of the first LM-IRSL measurement is simulated using equation (22). Since the duration of each measurement in Fig. 6(a) is 400 s, the distribution of remaining electrons $n_g(r',t)$ at the end of the first LM-IRSL measurement is calculated using equation (22) with time $t = 400$ s. This distribution $n_g(r',t{=}400s)$ is used as the *initial* distribution $n_g(r',0)$ of electrons the second LM-IRSL measurement. By using this new initial distribution as $n_g(r',0)$ in equation (11), the time variation of $n_g(r',t)$ and the corresponding luminescence intensity $L(t)$ can be calculated as outlined previously, and yields the solid curve 2 in Fig. 6(a). This complete simulation procedure is repeated *for each new measurement cycle*, by estimating the new initial distribution of electrons $n_g(r',0)$, the time variation of $n_g(r',t)$ and the corresponding luminescence intensity $L(t)$ 15 times, with the results shown as solid lines in Figure 6(a) and 6(b). Once more, reasonably good agreement is seen between the simulation and the experimental data.

5. Conclusions

In this paper it was shown that the time dependence of the system of differential equations developed by Jain et al. (2012) can be partially integrated analytically, by using certain physical approximations for the excited state of the donor–acceptor system. By integrating explicitly the time dependence it is possible to obtain expressions for the distribution of donors in the ground state as a function of time and distance, for several possible modes of stimulation, namely TL, OSL, LM-OSL, LM-IRSL and isothermal TL.

It was demonstrated how typical LM-IRSL signals can be analyzed using the model of random defects interacting via the tunneling mechanism, and what physical information can be extracted from such experimental data. The equations developed in this paper were tested by fitting a series of experimental LM-IRSL data for Na- and K-feldspar samples available in the literature. Furthermore, it was shown that the equations derived in this paper are a generalization of the equation derived by Huntley (2006) for the case of ground state tunneling.

The simulations in this paper provide strong evidence that LM-IRSL signals from at least some types of preheated feldspar samples may consist of a single component, instead of the usual assumption made by researchers that these signals contain three first order components with distinct optical cross sections.

Clearly further experimental work needs to be carried out with different types of thermal and optical treatments of feldspar samples, in order to ascertain whether the conclusions drawn from the model apply to other types of samples.

References

Andersen, M.T., Jain, M., Tidemand-Lichtenberg, P., 2012. Red-IR stimulated luminescence in K-feldspar: single or multiple trap origin? J. Appl. Phys. 112, 043507.

Ankjærgaard, C., Jain, M., Kalchgruber, R., Lapp, T., Klein, D., McKeever, S.W.S., Murray, A.S., Morthekai, P., 2009. Further investigations into pulsed optically stimulated luminescence from feldspars using blue and green light. Radiat. Meas. 44, 576–581.

Bailiff, I.K., Poolton, N.R.J., 1991. Studies of charge transfer mechanisms in feldspars. Nucl. Tracks Radiat. Meas. 18, 111–118.

Baril, M.R., 2002. Spectral Investigations of Luminescence in Feldspars. Ph.D. thesis. Simon Fraser University, Burnaby, BC, Canada. Available online at: www.cfht.hawaii.edu/wbaril/Temp/baril_phdthesis.pdf.

Baril, M.R., Huntley, D.J., 2003. Optical excitation spectra of trapped electrons in irradiated feldspars. J. Phys. Cond. Matt. 15, 8011–8027.

Bøtter-Jensen, L., McKeever, S.W.S., Wintle, A.G., 2003. Optically Stimulated Luminescence Dosimetry. Elsevier, Amsterdam.

Bøtter-Jensen, L., Duller, G.A.T., Poolton, N.R.J., 1994. Excitation and emission spectrometry of stimulated luminescence properties of feldspars. Radiat. Meas. 23, 613–616.

Bull, R.K., 1989. Kinetics of the localised transition model for thermoluminescence. J. Phys. D: Appl. Phys. 22, 1375–1379.

Bulur, E., Goksu, H.Y., 1999. Infrared (IR) stimulated luminescence from feldspars with linearly increasing excitation light intensity. Radiat. Meas. 30, 505–512.

Chen, R., McKeever, S.W.S., 1997. Theory of Thermoluminescence and Related Phenomena. World Scientific, Singapore.

Chen, R., Pagonis, V., 2011. Thermally and Optically Stimulated Luminescence: a Simulation Approach. Wiley and Sons, Chichester.

Chen, R., Lawless, J.L., Pagonis, V., 2012. Two-stage thermal stimulation of thermoluminescence. Radiat. Meas. 47, 809–813.

Chen, R., 1976. Methods for kinetics analysis of thermally stimulated processes. J. Mater. Sci. 11, 1521–1541.

Delbecq, C.J., Toyozawa, Y., Yuster, P.H., 1974. Tunneling recombination of trapped electrons and holes in KCl: AgCl and KCl: TlCl. Physiol. Rev. B9, 4497–4505.
Duller, G.A.T., Bøtter-Jensen, L., 1993. Luminescence from potassium feldspars stimulated by infrared and green light. Radiat. Prot. Dosimetry 47, 683–688.
Duller, G.A.T., 1997. Behavioural studies of stimulated luminescence from feldspars. Radiat. Meas. 27, 663–694.
Fattahi, M., Singarayer, J.S., Bailey, R.M., Stokes, S., 2006. The linearly modulated IRSL red emission from feldspars. Geochronometria 25, 19–28.
Fattahi, M., Stokes, S., 2003. Red luminescence from potassium feldspar for dating applications: a study of some properties relevant for dating. Radiat. Meas. 37, 647–660.
Huntley, D.J., Lamothe, M., 2001. Ubiquity of anomalous fading in K-feldspars and the measurement and correction for it in optical dating. Can. J. Earth Sci. 38, 1093–1106.
Huntley, D.J., 2006. An explanation of the power-law decay of luminescence. J. Phys. Cond. Matt. 18, 1359–1365.
Hutt, G., Jaek, I., Tchonka, J., 1988. Optical dating: K-feldspars' optical response stimulation spectrum. Quat. Sci. Rev. 7, 381–386.
Hutt, G., Jaek, I., 1993. Photostimulated luminescence of some materials and its dosimetry applications. Nucl. Tracks Radiat. Meas. 21, 95–98.
Jain, M., Guralnik, B., Andersen, M.T., 2012. Stimulated luminescence emission from localized recombination in randomly distributed defects. J. Phys. Condens. Matter 24, 385402 (12pp.).
Jain, M., Ankjærgaard, C., 2011. Towards a non-fading signal in feldspar: insight into charge transport and tunneling from time-resolved optically stimulated luminescence. Radiat. Meas. 46, 292–309.
Kitis, G., Pagonis, V., 2013. Analytical solutions for stimulated luminescence emission from tunneling processes in random distributions of defects. J. Lum. 137, 109–115.
Kumar, M., Kher, R.K., Bhatt, B.C., Sunta, C.M., 2006. Thermally stimulated luminescence arising simultaneously from localized and delocalized recombination processes. J. Phys. D: Appl. Phys. 39, 2670–2679.
Kumar, M., Kher, R.K., Bhatt, B.C., Sunta, C.M., 2007. A comparative study of the models dealing with localized and semi-localized transitions in thermally stimulated luminescence. J. Phys. D: Appl. Phys. 40, 5865–5872.
Kars, R.H., Wallinga, J., Cohen, K.M., 2008. A new approach towards anomalous fading correction for feldspar IRSL dating-tests on samples in field saturation. Radiat. Meas. 43, 786–790.
Larsen, A., Greilich, S., Jain, M., Murray, A.S., 2009. Developing a numerical simulation for fading in feldspar. Radiat. Meas. 44, 467–471.
Li, B., Li, S.-H., 2010. Thermal stability of infrared stimulated luminescence of sedimentary K-feldspar. Radiat. Meas. 46, 29–36.
Li, B., Li, S.-H., 2008. Investigations of the dose-dependent anomalous fading rate of feldspar from sediments. J. Phys. D: Appl. Phys. 41, 225502.
Mandowski, A.J., 2005. Semi-localized transitions model for Thermoluminescence. Phys. D: Appl. Phys. 38, 17–21.
Murray, A.S., Buylaert, J.P., Thomsen, K.J., Jain, M., 2009. The effect of preheating on the IRSL signal from feldspar. Radiat. Meas. 44, 554–559.
Pagonis, V., Jain, M., Murray, A.S., Ankjærgaard, C., Chen, R., 2012. Modeling of the shape of infrared stimulated luminescence signals in feldspars. Radiat. Meas. 47, 870–876.
Poolton, N.R.J., Wallinga, J., Murray, A.S., Bulur, E., Bøtter-Jensen, L., 2002a. Electrons in feldspar I: on the wave function of electrons trapped at simple lattice defects. Phys. Chem. Minerals 29, 210–216.
Poolton, N.R.J., Ozanyan, K.B., Wallinga, J., Murray, A.S., Bøtter-Jensen, L., 2002b. Electrons in feldspar II: a consideration of the influence of conduction band-tail states on luminescence processes. Phys. Chem. Minerals 29, 217–225.
Poolton, N.R.J., Kars, R.H., Wallinga, J., Bos, A.A.J., 2009. Direct evidence for the participation of band-tails and excited-state tunneling in the luminescence of irradiated feldspars. J. Phys. Cond. Matt. 21, 485505.
Sunta, C.M., Kumar, M., Kher, R.K., Bhatt, B.C., 2006. Thermoluminescence emission from localized recombination model. J. Phys. D: Appl. Phys. 39, 4557–4562.
Templer, R.H., 1986. The localized transition model of anomalous fading. Radiat. Prot. Dosimetry 17, 493–497.
Thomsen, K.J., Murray, A.S., Jain, M., Bøtter-Jensen, L., 2008. Laboratory fading rates of various luminescence signals from feldspar-rich sediment extracts. Radiat. Meas. 43, 1474–1486.
Thomsen, K.J., Murray, A.S., Jain, M., 2011. Stability of IRSL signals from sedimentary K-feldspar samples. Geochronometria 38, 1–13.
Visocekas, R., 1985. Tunnelling radiative recombination in labradorite; its association with anomalous fading of thermoluminescence. Nucl. Tracks Radiat. Meas. 10, 149–154.
Visocekas, R., Spooner, N.A., Zink, A., Blank, P., 1994. 1994. Tunnel afterglow, fading and infrared emission in thermoluminescence of feldspars. Radiat. Meas. 23, 377–385.